



**HAL**  
open science

# Fabrication of Tapered and Cylindrical GaN Nanowires Using Nanosphere Lithography

Elçin Akar, Bruno César da Silva, Matteo Knebel, Martien den Hertog, Eva  
Monroy

► **To cite this version:**

Elçin Akar, Bruno César da Silva, Matteo Knebel, Martien den Hertog, Eva Monroy. Fabrication of Tapered and Cylindrical GaN Nanowires Using Nanosphere Lithography. 2024 IEEE 24th International Conference on Nanotechnology (NANO), Jul 2024, Gijon, Spain. pp.86-90, 10.1109/NANO61778.2024.10628950 . hal-04765849

**HAL Id: hal-04765849**

**<https://hal.science/hal-04765849v1>**

Submitted on 4 Nov 2024

**HAL** is a multi-disciplinary open access archive for the deposit and dissemination of scientific research documents, whether they are published or not. The documents may come from teaching and research institutions in France or abroad, or from public or private research centers.

L'archive ouverte pluridisciplinaire **HAL**, est destinée au dépôt et à la diffusion de documents scientifiques de niveau recherche, publiés ou non, émanant des établissements d'enseignement et de recherche français ou étrangers, des laboratoires publics ou privés.

This document is the unedited Author's version post review of a Submitted Work that was subsequently accepted for publication in 2024 IEEE 24th International Conference on Nanotechnology (NANO), Gijon, Spain, 2024, pp. 86-90, doi: 10.1109/NANO61778.2024.10628950, after peer review. To access the final edited and published work see [<https://ieeexplore.ieee.org/abstract/document/10628950>].

# Fabrication of tapered and cylindrical GaN nanowires using nanosphere lithography

Elçin Akar, Bruno César Da Silva, Matteo Knebel, Martien den Hertog, Eva Monroy

**Abstract**—Nanowires fabricated using the top-down method can offer high uniformity and precise morphology. However, achieving well-controlled dry and wet etching processes is essential to produce large-area uniform nanowires. It is also interesting to have control on their shape, since tapered structures can have favorable light extraction properties, whereas cylindrical shapes are preference for electronics or photodetection. This paper presents a comprehensive study on the fabrication of GaN nanowires using a top-down approach facilitated by nanosphere lithography. We focus on optimizing both dry and wet etching processes to achieve high-aspect-ratio nanowires with controlled shapes. The final wet etching step, critical for shaping the nanowires, was performed with a crystallography-selective method, resulting in nanowires with vertical *m*-plane facets or tapered structures, depending on the initial diameter of the spheres. This demonstrates the process's adaptability to control nanowire geometry.

## I. INTRODUCTION

GaN nanowires have gained significant interest in the field of nanotechnology and materials science due to their exceptional properties and versatile applications. These nanowires exhibit direct band gap, high robustness and chemical stability, making them highly efficient for optoelectronic devices, including light-emitting diodes (LEDs) [1], [2], laser diodes [3], and ultraviolet (UV) photodetectors [4], [5], [6], [7]. Nanowire devices offer lower capacitance, enhanced integration, and excellent spectral selectivity compared to planar devices [8]. The ability to tailor their optical and electronic properties through size, shape, heterostructure and doping adjustments further enhances their appeal for innovative nanoscale device applications.

Two methods can be employed for fabricating vertically aligned nanowires: bottom-up growth (which includes self-assembly, selective area growth, or metal-seeded growth) and top-down fabrication of nanowires from planar layers. Nanowires grown via the bottom-up approach display an almost defect-free structure and enable the combination of different lattice parameters due to surface relaxation through the sidewalls. However, this method also presents drawbacks such as nonuniform doping and defect formation associated with nanowire coalescence [9]. Conversely, the top-down method holds the promise of enhanced uniformity, better nanowire morphology, and better doping control with respect to bottom-up method [10]. To fabricate top-down GaN

nanowires, different methods have been employed. For instance electron beam lithography can be used for the definition of the nanowire diameter and periodicity, coupled with additional processes such as dry and wet etching steps [11] or selective area sublimation [12], but the exposure time can be long and it is not easily scalable. Nanosphere lithography has emerged as a promising method for top-down fabrication, because it allows controlling the nanowire diameter and length, and it is scalable [13]. Recently, a novel approach has been developed by da Silva *et al.* [9] in which they reported using polystyrene spheres in combination with a SiO<sub>2</sub> layer to pattern the nanowires employing both dry and wet etching to provide large area thin GaN NWs with an aspect-ratio higher than 30.

In this study, we propose a cost-friendly and reproducible top-down process using nanosphere lithography with SiO<sub>2</sub> as a hard mask, which is applied to GaN samples grown by plasma-assisted molecular beam epitaxy (PAMBE). The dry etching step of the process for nanowire formation has been revised to achieve anisotropic etching, resulting in well-separated nanowires. Moreover, selecting the size of the spheres, it is possible to obtain nanowires either with vertical facets or tapered nanowires.

## II. EXPERIMENTAL PROCEDURE

GaN layers were grown using PAMBE on 4- $\mu$ m-thick non-intentionally-doped (nid) GaN-on-sapphire templates. The nitrogen plasma source was operated at 300 W radio-frequency (RF) power, with 1 sccm N<sub>2</sub> flow rate. The nitrogen-limited growth rate was 0.66 monolayers per second (ML/s). The samples used for dry etching optimization consisted of 600 nm of nid GaN (results shown in Fig. 2). The samples that underwent the complete NW fabrication process consisted of 600 nm GaN:Mg (results shown in Fig. 3 and 4). The sphere shrinking step is performed in a Plassy reactive ion etching (RIE) equipment, whereas the etching of SiO<sub>2</sub> and GaN was performed in an Oxford Plasmalab System100 inductively coupled plasma-reactive ion etching (ICP-RIE) equipment. The samples were examined by scanning electron microscopy (SEM) throughout the complete fabrication process.

Elçin Akar is the corresponding author and with Univ. Grenoble-Alpes, CEA, Grenoble INP, IRIG, PHELIQS, 38000 Grenoble, France (e-mail: elcin.akar@cea.fr). Bruno César Da Silva, Matteo Knebel, and Martien den Hertog are with Univ. Grenoble-Alpes, CNRS, Grenoble INP, Institut Néel, 38000 Grenoble, France (e-mail: martien.den-hertog@neel.cnrs.fr). Eva

Monroy is with Univ. Grenoble-Alpes, CEA, Grenoble INP, IRIG, PHELIQS, 38000 Grenoble, France (e-mail: eva.monroy@cea.fr).

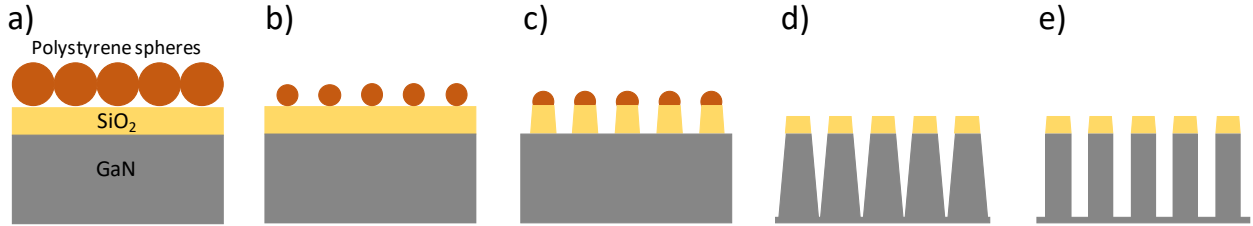


Figure 1. Schematic description of the top-down NW fabrication process a) dispersion of polystyrene spheres on the SiO<sub>2</sub>/GaN specimen, b) shrinking the polystyrene spheres, c) etching the SiO<sub>2</sub> layer, d) dry etching of GaN using the patterned geometry, and e) wet etching of GaN nanowires to smooth the sidewalls.

### III. DISCUSSION

Our target is to obtain high-aspect-ratio nanowires using a top-down fabrication process, with a pattern generated via nanosphere lithography. For this purpose, we selected polystyrene spheres as the lithographic medium, since we have previously developed a process that uniformly reduces their diameter without deformation, using oxygen plasma in a RIE system [9]. This technique ensures a good separation between spheres, but the selectivity of the GaN etching chemistry is insufficient to use the spheres directly as a mask. Consequently, we need to deposit a SiO<sub>2</sub> layer, whose pattern is defined by the spheres, which serves as a hard mask for the etching of GaN. Following this reasoning, this paper describes a nanosphere lithography process that follows the steps depicted in Fig. 1, including a) dispersion of polystyrene spheres on the SiO<sub>2</sub>/GaN specimen, b) shrinking the polystyrene spheres to separate them, c) etching the SiO<sub>2</sub> layer, d) dry etching of GaN using the patterned SiO<sub>2</sub> as a mask, and e) wet etching of the GaN rods to obtain nanowires with vertical and smooth sidewalls.

The fabrication protocol started with the deposition of a SiO<sub>2</sub> layer with a thickness of 700 nm, using plasma-enhanced chemical vapor deposition (PECVD). Then, a colloidal solution of polystyrene spheres with a diameter of 1 μm was deposited onto the sample. The spheres, initially provided in an aqueous suspension (2% solids), are highly hydrophobic, leading to a predisposition to clustering [14]. To achieve a homogeneous solution of spheres on the sample surface, the suspension underwent sonication for approximately 30 min. Then, a solution was prepared using water and the sphere suspension at a 2:1 volume ratio. The solution was deposited onto the sample using a drop-casting wet dispersion method with the substrate mounted on a 10° inclined sample holder. A 30 μl droplet of the solution was applied to a specimen with a surface of 5 mm × 5 mm. After dispersion, the sample was left to dry for one hour.

To create some spacing between the spheres, they were etched with oxygen plasma in a RIE system (O<sub>2</sub> flow = 50 sccm, RF power = 100 W, pressure in the chamber =

0.070 mbar) to reach a diameter around 550 nm. Using the shrunk spheres as a mask, the SiO<sub>2</sub> layer was etched in an ICP-RIE system with CF<sub>4</sub>/Ar/CH<sub>2</sub>F<sub>2</sub> chemistry (20/50/5 sccm, RF power = 500 W, ICP power = 0 W, pressure in the chamber = 12 mTorr).

After the hard mask opening step, the GaN was dry etched using ICP-RIE with a Cl<sub>2</sub>-based chemistry. We have evaluated multiple etching protocols, summarized in Table I, aimed at enhancing the verticality of the etched sidewalls. Note that the etching angle (angle between the etched sidewalls and the direction normal to the sample surface) determines the maximum length achievable for the nanowires.

The BC1 recipe in Table I, which uses BCl<sub>3</sub>/Cl<sub>2</sub> chemistry, was derived from ref. [9]. Fig. 2a presents an SEM image of a sample after 2 hours of etching, resulting in ≈1.2 μm long GaN pillars, which corresponds to an etching rate of 10 nm/min. Unfortunately, the etching angle is so large that the GaN rods converge at a depth of 1 μm.

Increasing the ICP power should result in a higher reactive ion flux, potentially facilitating more anisotropic etching, whereas increasing the RF power should lead to higher etching rate [15]. Hence, we adjusted the CB1 recipe by increasing both the RF and ICP power settings (recipe CB2 in Table I). Fig. 2b depicts the outcome of the new recipe after 10 min of etching. Despite the anticipated increase in etching rate (65 nm/min), the etching angle was comparable or even larger than the one in Fig. 2a.

In a new effort to improve the sidewall verticality, we decided to change the etching chemistry to pure Cl<sub>2</sub>, using the C1 recipe in Table I. The SEM image in Fig. 2c, after 10 min of etching with this recipe, reveal a negligible GaN etching rate. However, by augmenting the ICP power to 990 W (as per recipe C2 in Table I), we achieved substantial etching rates of 300 nm/min, as depicted in Fig. 2d following 10 min of etching.

These experiments demonstrate the efficacy of using pure Cl<sub>2</sub> for deep etching of GaN, facilitating high etch rates, while maintaining small etching angles. This conclusion aligns with the observations of Jaloustre *et al.* [16], reinforcing the

TABLE I. ICP-RIE recipes applied in this study.

Recipe	Chemistry	Flow Ratio (sccm)	RF Power (W)	ICP Power (W)	Pressure (mTorr)	Temperature (°C)
BC1	BCl <sub>3</sub> /Cl <sub>2</sub>	30/10	30	100	10	20
BC2	BCl <sub>3</sub> /Cl <sub>2</sub>	30/10	300	1000	10	20
C1	Cl <sub>2</sub>	80	100	400	8	20
C2	Cl <sub>2</sub>	80	100	990	8	20

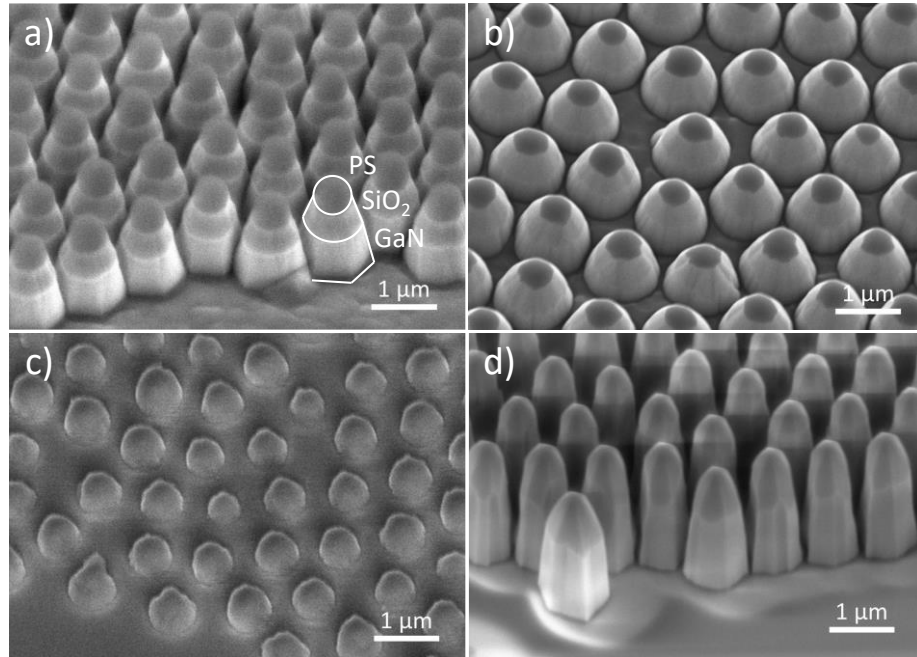


Figure 2. SEM images of GaN dry etching study after using different ICP-RIE recipes a) BC1, b) BC2, c) C1, and d) C2 (All images are tilted with 30°).

preference for pure  $\text{Cl}_2$  over  $\text{BCl}_3/\text{Cl}_2$  in applications requiring deep etching of GaN.

Following the dry etching process, which transformed the GaN layer into 2  $\mu\text{m}$  long rods, the samples underwent wet etching at 65°C in AZ400K developer (KOH-based developer from AZ Electronic Materials USA Corp.). Fig. 3a shows that after 10 min of wet etching, the formation of nanowires with a diameter of approximately 200 nm is already evident. Additional etching steps reveal non-uniform etching of the nanowires (Figs. 3b and 3c). Furthermore, the nanowire geometry transitions from cylindrical to conical reminds the report of Kazanowska *et al.* [17] of tapered GaN nanowires resulting from crystallographic wet etching using phosphoric acid. This process was found to be crystallographically sensitive in nature, with semipolar planes exposed rather than nonpolar planes. To our knowledge, a nanowire geometry with sharp tips has not been previously reported when using KOH as a wet etchant, which is known to expose  $m\text{-}\{10\text{-}10\}$  facets [18], [19], [20], [21]. Note that these GaN nanowires with sharp tips could find utility in scanning probe microscopy or field emission devices.

To obtain cylindrical nanowires with controlled height, we need to adapt the process to spheres with a larger diameter. Therefore, polystyrene spheres with a diameter of 2  $\mu\text{m}$  were dispersed and etched under the same oxygen plasma conditions (RIE with  $\text{O}_2$  flow = 50 sccm, RF power = 100 W, pressure in the chamber = 0.070 mbar) until their diameter reduces to approximately 1.35  $\mu\text{m}$ , with a pitch size of 600 nm. Following the  $\text{SiO}_2$  etching (ICP-RIE with  $\text{CF}_4/\text{Ar}/\text{CH}_2\text{F}_2$  20/50/5 sccm, RF power = 500 W, ICP power = 0 W, pressure in the chamber = 12 mTorr), GaN was etched using the C2 recipe in Table I, to obtain 2  $\mu\text{m}$  long rods, which were subsequently wet etched. Fig. 4 illustrates the evolution of the sidewall facets during wet etching. The areas damaged during dry etching are quickly eliminated, as observed in Fig. 4a

which shows the state of the sample after 10 min of etching. After 30 min (Fig. 4b), the vertical  $m\text{-}\{10\text{-}10\}$  facets start to appear at the upper portion of the structures, whereas the lower section exhibits nanofacets, mostly  $c\text{-}(0001)$  and  $m\text{-}\{10\text{-}10\}$  planes. Further increasing the etching time (Fig. 4c), the vertical facets become larger and the presence of (0001) nanofacets is restricted to the region closer to substrate. For longer etching time (Fig. 4d), the nanowires present a cylindrical shape with vertical sidewalls and a flat top facet. Once such a profile is obtained, the rate of decrease in nanowire diameter depends on the etching time.

Let us remind here that the process began with a shrunk-sphere diameter of 1.35  $\mu\text{m}$ . After wet etching for 10 min, the top-facet diameter reduces to 1  $\mu\text{m}$  due to the rapid elimination of the material damaged during the ICP-RIE process. From there, the evolution of the diameter of the top facet as a function of the etching time is given in Fig. 4e. In a

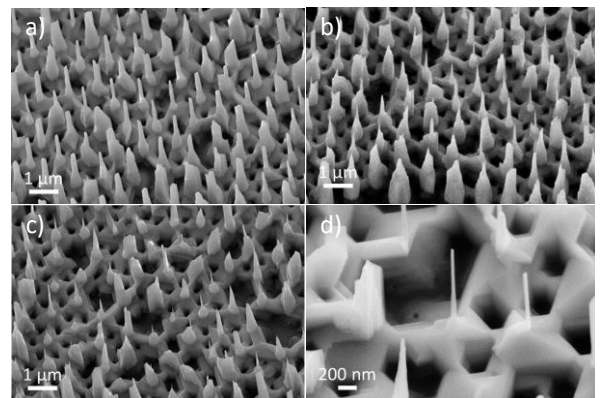


Figure 3. SEM images of wet etching study with 1  $\mu\text{m}$  spheres in AZ400 solution for a) 10 min, b) 12 min, c) 14, and d) 17 min. (All images are tilted with 30°).



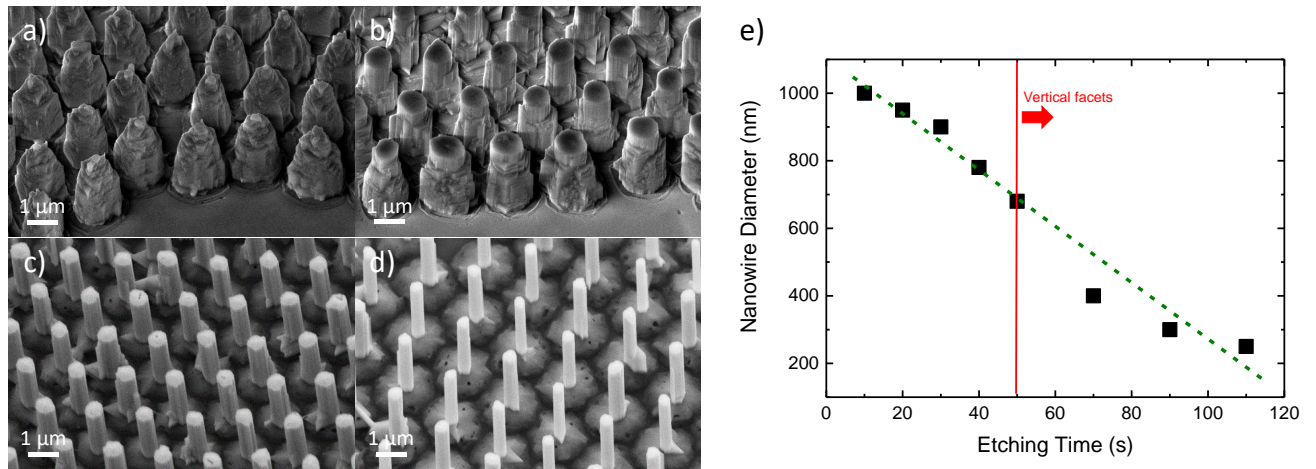


Figure 4. SEM images of the wet etching study with 2  $\mu\text{m}$  spheres in AZ400 solution for a) 10 min, b) 30 min, c) 50 min, d) 90 min (All images are tilted 30°). e) Nanowire diameter as a function of the wet etching time. The dashed line represents the linear behavior.

first approximation, after the first 10 min, the diameter decreases linearly with time. The vertical *m*-plane facets get fully exposed after 50 min, when the top facet diameter is around 700 nm.

The process is schematically described in Fig. 5 for the two tested sphere diameters. This evolution explains the tapered geometry of the nanowires fabricated using 1  $\mu\text{m}$  spheres, Fig. 5a. In that situation, the sphere diameter was approximately 550 nm after oxygen plasma etching, and after 10 minutes of wet etching, the diameter of the nanowire top facet had decreased to 200 nm. In the case of 2  $\mu\text{m}$  spheres, Fig. 5b, the diameter reduced from 1.35  $\mu\text{m}$  to 1  $\mu\text{m}$ . This implies a difference of 350 nm between the diameter of the shrunk spheres and that of the nanowire top facet after 10 min of wet etching, regardless of the initial sphere diameter. In the case of the small spheres, with only 200 nm as initial point for the top facet, the nanowires will start losing height before attaining the point that leads to fully vertical facets. This diminishment occurs because the top facet's size is insufficient to prevent lateral etching. Therefore, inclined facets appear at the nanowire tip and can subsequently be further etched. As a result, we obtain a tapered structure instead of a cylindrical shape and lose nanowire height reducing the aspect ratio of the fabricated structures.

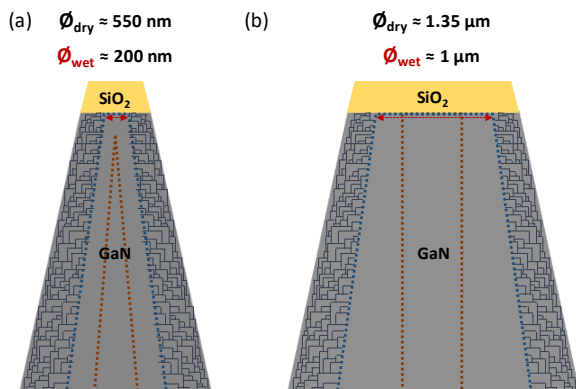


Figure 5. Schematic description of wet etching profile of samples prepared with a) 1  $\mu\text{m}$  spheres and b) 2  $\mu\text{m}$  spheres. Orange dashed lines illustrate the final shape of the nanowires.

#### IV. CONCLUSION

In conclusion, we have successfully developed a top-down process for the fabrication of GaN nanowires, using nanosphere lithography. Our results indicate a clear preference for employing pure  $\text{Cl}_2$  chemistry over  $\text{BCl}_3\text{-Cl}_2$  mixtures for the deep etching of GaN via ICP-RIE, a critical step that ensures the production of well-separated nanowires with high aspect ratios. The final crystallographic-selective wet etching step facilitates the formation of vertical nanowires with *m*-plane facets or tapered structures, depending on the initial diameter of the spheres. In summary, we demonstrate that the use polystyrene spheres with  $\text{SiO}_2$  as a mask, coupled with meticulous adjustments in dry and wet etching steps, renders the top-down GaN nanowire fabrication process more reliable and allows controlling the nanowire shape.

#### ACKNOWLEDGMENT

This work was partially supported by French National Research Agency via the INMOST project (ANR-19-CE08-0025) and received funding from the European Research Council under the European Union's H2020 Research and Innovation programme via the e-See project (Grant No. 758385). A CC-BY public copyright license has been applied by the authors to the present document and will be applied to all subsequent versions up to the Author Accepted Manuscript arising from this submission, in accordance with the grant's open access conditions. The authors would like to thank to the Néel Institute Nanofab and CEA Upstream Technological Platform (PTA) clean room teams for their technical support during the fabrication steps.

## REFERENCES

- [1] M. Z. Baten, S. Alam, B. Sikder, and A. Aziz, "III-Nitride Light-Emitting Devices," *Photonics*, vol. 8, no. 10, p. 430, Oct. 2021, doi: 10.3390/photonics8100430.
- [2] M. Žak, "Bidirectional light-emitting diode as a visible light source driven by alternating current," *Nat. Commun.*, vol. 14, no. 7562, 2023, doi: <https://doi.org/10.1038/s41467-023-43335-7>.
- [3] M. Behzadrad *et al.*, "Scalable Top-Down Approach Tailored by Interferometric Lithography to Achieve Large-Area Single-Mode GaN Nanowire Laser Arrays on Sapphire Substrate," *ACS Nano*, vol. 12, no. 3, pp. 2373–2380, Mar. 2018, doi: 10.1021/acsnano.7b07653.
- [4] Q. Cai *et al.*, "Progress on AlGaIn-based solar-blind ultraviolet photodetectors and focal plane arrays," *Light Sci. Appl.*, vol. 10, no. 1, p. 94, Apr. 2021, doi: 10.1038/s41377-021-00527-4.
- [5] L. Peng, L. Hu, and X. Fang, "Low-Dimensional Nanostructure Ultraviolet Photodetectors," *Adv. Mater.*, vol. 25, no. 37, pp. 5321–5328, Oct. 2013, doi: 10.1002/adma.201301802.
- [6] E. Akar, I. Dimkou, A. Ajay, E. Robin, M. I. den Hertog, and E. Monroy, "GaN and AlGaIn/AlN Nanowire Ensembles for Ultraviolet Photodetectors: Effects of Planarization with Hydrogen Silsesquioxane and Nanowire Architecture," *ACS Appl. Nano Mater.*, vol. 6, no. 14, pp. 12792–12804, Jul. 2023, doi: 10.1021/acsnm.3c01496.
- [7] S. Cuesta *et al.*, "Effect of Bias on the Response of GaN Axial p–n Junction Single-Nanowire Photodetectors," *Nano Lett.*, vol. 19, no. 8, pp. 5506–5514, Aug. 2019, doi: 10.1021/acs.nanolett.9b02040.
- [8] Y. Zou, Y. Zhang, Y. Hu, and H. Gu, "Ultraviolet Detectors Based on Wide Bandgap Semiconductor Nanowire: A Review," *Sensors*, vol. 18, no. 7, p. 2072, Jun. 2018, doi: 10.3390/s18072072.
- [9] B. C. Da Silva *et al.*, "High-Aspect-Ratio GaN p–i–n Nanowires for Linear UV Photodetectors," *ACS Appl. Nano Mater.*, vol. 6, no. 14, pp. 12784–12791, Jul. 2023, doi: 10.1021/acsnm.3c01495.
- [10] B. Melanson, M. Hartensveld, C. Liu, and J. Zhang, "Realization of electrically driven AlGaIn micropillar array deep-ultraviolet light emitting diodes at 286 nm," *AIP Adv.*, vol. 11, no. 9, p. 095005, Sep. 2021, doi: 10.1063/5.0061381.
- [11] M. Oliva *et al.*, "A route for the top-down fabrication of ordered ultrathin GaN nanowires," *Nanotechnology*, vol. 34, no. 20, p. 205301, May 2023, doi: 10.1088/1361-6528/acb949.
- [12] S. Fernández-Garrido, T. Auzelle, J. Lähnemann, K. Wimmer, A. Tahraoui, and O. Brandt, "Top-down fabrication of ordered arrays of GaN nanowires by selective area sublimation," *Nanoscale Adv.*, vol. 1, no. 5, pp. 1893–1900, 2019, doi: 10.1039/C8NA00369F.
- [13] T. Granz *et al.*, "Nanofabrication of Vertically Aligned 3D GaN Nanowire Arrays with Sub-50 nm Feature Sizes Using Nanosphere Lift-off Lithography," in *Proceedings of Euroensors 2017, Paris, France, 3–6 September 2017*, MDPI, Aug. 2017, p. 309. doi: 10.3390/proceedings1040309.
- [14] M. Domonkos and A. Kromka, "Nanosphere Lithography-Based Fabrication of Spherical Nanostructures and Verification of Their Hexagonal Symmetries by Image Analysis," *Symmetry*, vol. 14, no. 2642, 2022, doi: <https://doi.org/10.3390/sym14122642>.
- [15] C.-C. Kao *et al.*, "Study of dry etching for GaN and InGaIn-based laser structure using inductively coupled plasma reactive ion etching," *Mater. Sci. Eng. B*, vol. 107, 2004, doi: 10.1016/j.mseb.2003.11.023.
- [16] L. Jaloustre, V. Ackermann, S. Sales De Mello, S. Labau, C. Petit-Etienne, and E. Pargon, "Preferential crystal orientation etching of GaN nanopillars in Cl<sub>2</sub> plasma," *Mater. Sci. Semicond. Process.*, vol. 165, p. 107654, Oct. 2023, doi: 10.1016/j.mssp.2023.107654.
- [17] B. A. Kazanowska *et al.*, "Fabrication and field emission properties of vertical, tapered GaN nanowires etched via phosphoric acid," *Nanotechnology*, vol. 33, no. 3, p. 035301, Jan. 2022, doi: 10.1088/1361-6528/ac2981.
- [18] M. Itoh, T. Kinoshita, C. Koike, M. Takeuchi, K. Kawasaki, and Y. Aoyagi, "Straight and Smooth Etching of GaN (1100) Plane by Combination of Reactive Ion Etching and KOH Wet Etching Techniques," *Jpn. J. Appl. Phys.*, vol. 45, no. 5R, p. 3988, May 2006, doi: 10.1143/JJAP.45.3988.
- [19] S. Cuesta, L. Denaix, F. Castioni, L. S. Dang, and E. Monroy, "Reduction of the lasing threshold in optically pumped AlGaIn/GaN lasers with two-step etched facets," *Semicond. Sci. Technol.*, vol. 37, no. 7, p. 075013, Jul. 2022, doi: 10.1088/1361-6641/ac7164.
- [20] W. Chen *et al.*, "GaN nanowire fabricated by selective wet-etching of GaN micro truncated-pyramid," *J. Cryst. Growth*, vol. 426, pp. 168–172, Sep. 2015, doi: 10.1016/j.jcrysgro.2015.06.007.
- [21] M. Hartensveld, G. Ouin, C. Liu, and J. Zhang, "Effect of KOH passivation for top-down fabricated InGaIn nanowire light emitting diodes," *J. Appl. Phys.*, vol. 126, no. 18, p. 183102, Nov. 2019, doi: 10.1063/1.5123171.